SUPPORTING INFORMATION FOR THE WORK

On the Enhanced Photocatalytic Activity of N-Doped Carbon Dots

Héctor Daniel Almeida,[1] Gabriel Rafael Guerrero Porras,[2] Hervé Vezin,[3] Lisandra Morales Alvarez,[3] Angel Luis Corcho Valdés,[3] Julieth Bravo Martínez,[4] Alicia M. Diaz Garcia,[2] David González-Martínez,[5] José Moran Mirabal,[5] Clarissa Murru,[6] Johnny Deschamps,[7] Claudia Iriarte-Mesa,[8,9] Qixiang Jiang,[10] Freddy Kleitz,[8] Luis Felipe Desdin Garcia,*[3] Manuel Antuch*[11]

[1] Instituto Superior de Tecnología y Ciencias Aplicadas (InSTEC), Universidad de La Habana, La Habana CP 10600, Cuba.
[2] Laboratorio de Bioinorgánica, Departamento de Química General e Inorgánica, Facultad de Química, Universidad de La Habana, La Habana, C.P. 10400, Cuba.
[3] Centro de Aplicaciones Tecnológicas y Desarrollo Nuclear (CEADEN), Miramar C.P. 11300, La Habana, Cuba.
[4] Centro de Estudios Avanzados de Cuba, La Habana, Cuba.
[5] Department of Chemistry and Chemical Biology, McMaster University, 1280 Main Street West, Hamilton, Ontario, L8S 4M1 Canada.
6 National Institute of Optics, National Research Council (INO-CNR), Via Nello Carrara 1, 50019 Sesto Fiorentino, Italy.
[7] Unité Chimie et Procédés (UCP), Ecole Nationale Supérieure de Techniques Avancées (ENSTA), Institut Polytechnique de Paris, 828 Boulevard des Maréchaux, 91120, Palaiseau, France.
[8] Department of Functional Materials and Catalysis, Faculty of Chemistry, University of Vienna, Währinger Str. 42, 1090 Vienna, Austria.
[9] Vienna Doctoral School in Chemistry (DoSChem), University of Vienna, Währinger Str. 42, 1090 Vienna, Austria.
[10] Institute of Material Chemistry and Research, Faculty of Chemistry, University of Vienna, Währinger Str. 42, 1090, Vienna.
[11] Univ. Lille, CNRS, Centrale Lille, Univ. Artois, UMR 8181, UCCS, Unité de Catalyse et Chimie du Solide, Lille F-59000, France.

*Luis Felipe Desdin-Garcia: luisfelipedesdingarcia@gmail.com
*Manuel Antuch: manuel.antuch@centralelille.fr

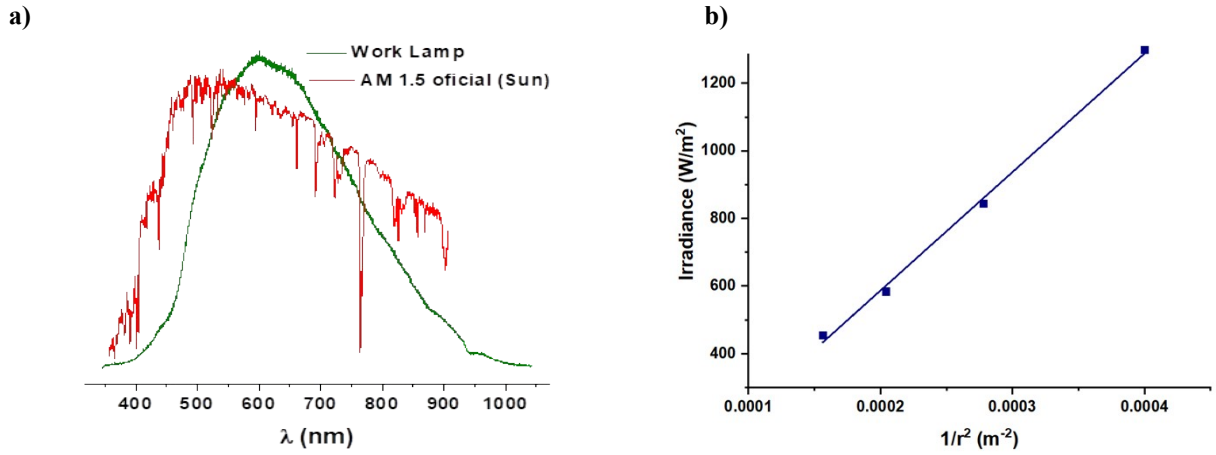

Figure S1. (a) Comparison of the work lamp and sunlight emission spectra. (b) Irradiance as a function of $1/r^2$.

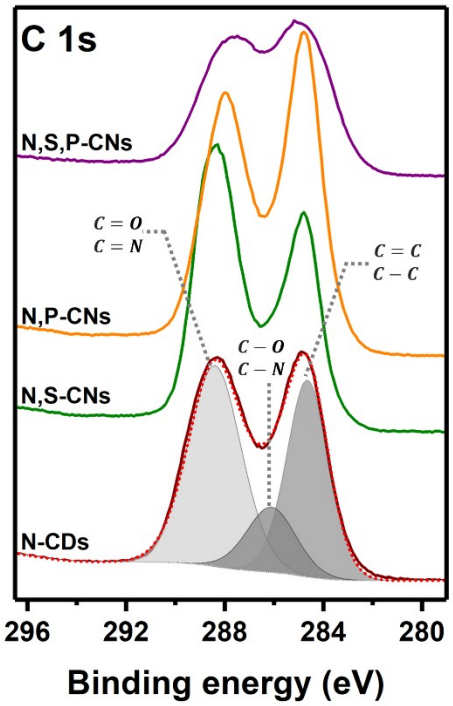

Figure S2. High-resolution X-ray photoelectron (XPS) spectra depicting C 1s orbital binding energy regions for doped carbon nanostructures.

Table S1. Elemental composition of doped carbon nanostructures obtained from XPS survey spectra.

Element	N-CDs		N,S-CNs		N,P-CNs		N,S,P-CNs	
	Binding Energy (eV)	Atomic %	Binding Energy (eV)	Atomic %	Binding Energy (eV)	Atomic %	Binding Energy (eV)	Atomic %
C	286.8	48.0	288.6	42.4	285.4	50.0	286.9	51.2
O	532.3	35.2	531.2	37.3	531.6	31.2	532.2	28.4
N	400.8	16.6	399.6	17.6	400.1	17.6	400.6	18.3
P	125.5	0.1	133.7	0.2	133.3	1.1	134.3	0.5
S	169.7	0.1	163.0	2.5	168.5	0.1	164.3	1.6

Table S2. Relative composition of different species of N, S and P present in doped carbon nanostructures obtained from XPS analysis.

Signal	Assignment	N-CDs		N,S-CNs		N,P-CNs		N,S,P-CNs	
		Binding Energy(eV)	Atomic %	Binding Energy (eV)	Atomic %	Binding Energy (eV)	Atomic %	Binding Energy (eV)	Atomic %
C 1s[1,2]	$C=O$; $C=N$	288.4	48.3	288.4	54.1	287.9	46.1	287.8	45.6
	$C-O$; $C-N$	286.1	14.5	286.3	12.0	285.7	13.1	286.1	8.2
	$C-C$; $C=C$	284.8	37.2	284.8	33.9	284.8 ($C-P$)	40.8	284.8 ($C-P$)	46.2
O 1s[2,3]	Na (Auger peak); $C-OH$	535.3	14.3	535.5	15.3	535.4	12.7	535.0	12.3
	$C-O-C$	532.2	13.6	532.4	8.3	532.3	10.4	532.2	7.9
	$C=O$	530.8	72.1	531.0	76.4	531.0	76.9	530.7	79.8
N 1s[2,4]	Pyrrolic (C_2-N-H)	399.5	69.8	399.5	79.2	399.5	79.9	399.2	88.6
	Pyridinic ($C=N-C$)	397.8	30.2	397.8	20.8	397.7	20.1	397.3	11.4
S 2p[5]	$-C-S-C-$ ($S2p_{3/2}$ and $S2p_{1/2}$)	-	-	162.8	66.2	-	-	162.9	72.0
	$-C-S^-$	-	-	161.2	33.8	-	-	161.2	28.0
P 2p[6]	P–O–C	-	-	-	-	132.8	100	132.8	100

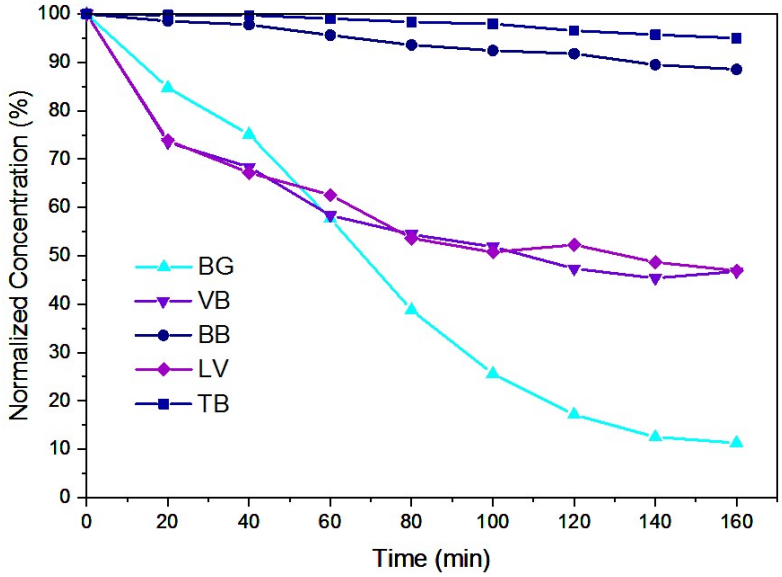

Figure S3. Comparison of dye photostabilities under visible light. Initial concentrations for each colorant where adjusted so that the absorbance range fell within the range where the Lambert-Beer law holds (0.2 – 0.8). The initial concentrations of the colorants were ρ(Brilliant Green) = 0.6 mg/mL (1.243×10^{-6} mol/L); ρ(Victoria Blue) = 7.0 mg/mL (1.528×10^{-5} mol/L); ρ(Brilliant Blue) = 3.0 mg/mL (3.632×10^{-6} mol/L); ρ(Lauth's Violet) = 7.0 mg/mL (2.654×10^{-5} mol/L) and

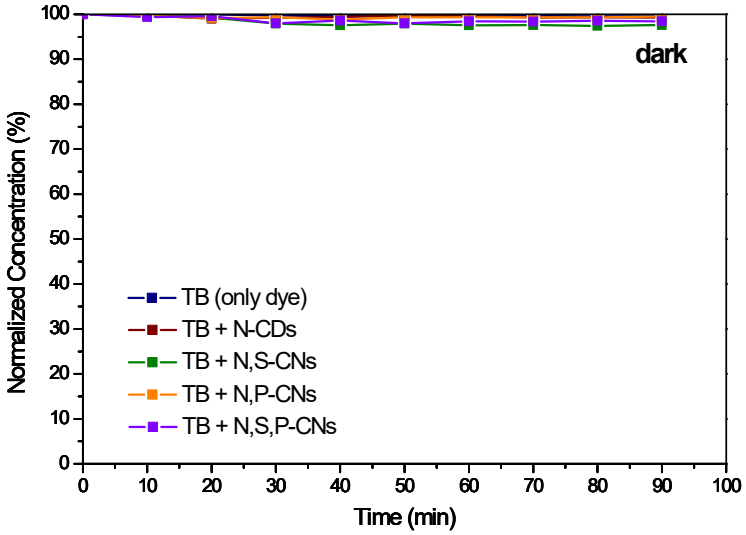

Figure S4. Time evolution of the normalized concentration of Toluidine Blue (TB, *ρ(TB) = 55* μg/mL *equals* c(TB) = $1.80 \cdot 10^{-7}$ M) in the presence of the doped nanostructures and without illumination.

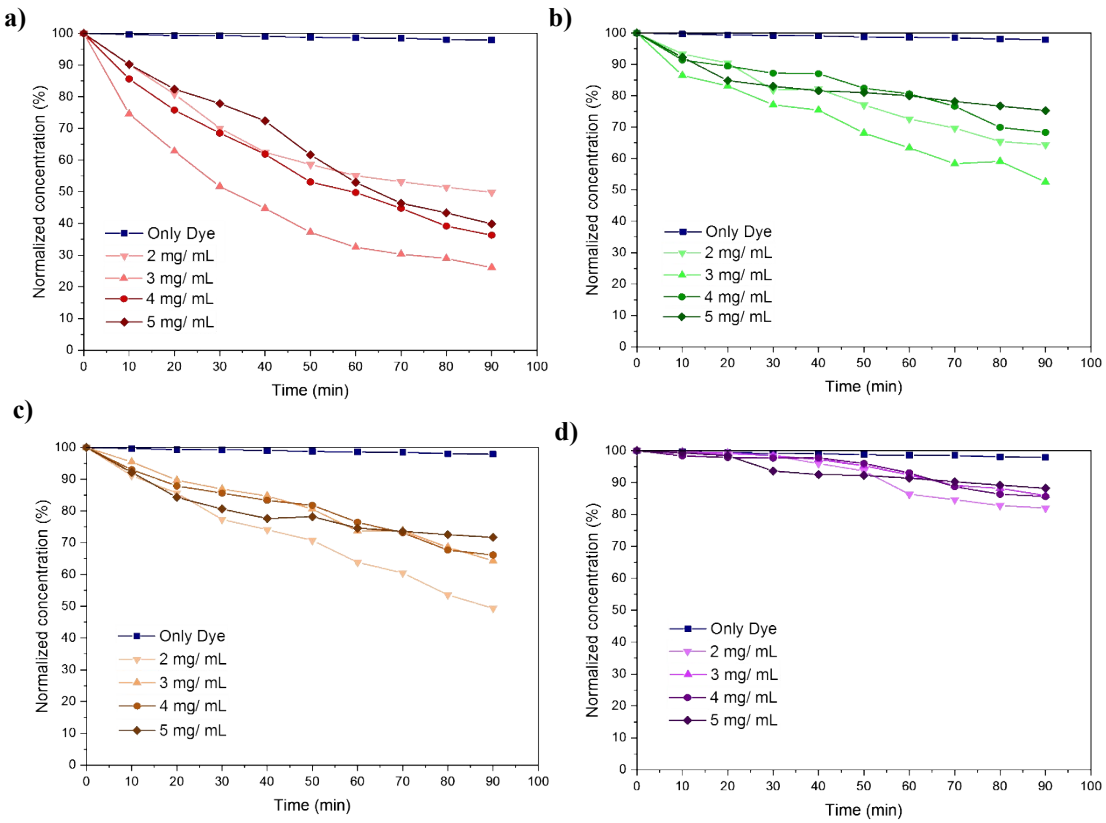

Figure S5. Time evolution of the normalized concentration of Toluidine Blue (TB, *ρ(TB) = 55 μg/mL equals c(TB) = 1.80·10⁻⁷ M*) in the presence of: (a) N-CDs; (b) N,S-CNs; (c) N,P-CNs; and (d) N,S,P-CNs at different concentrations.

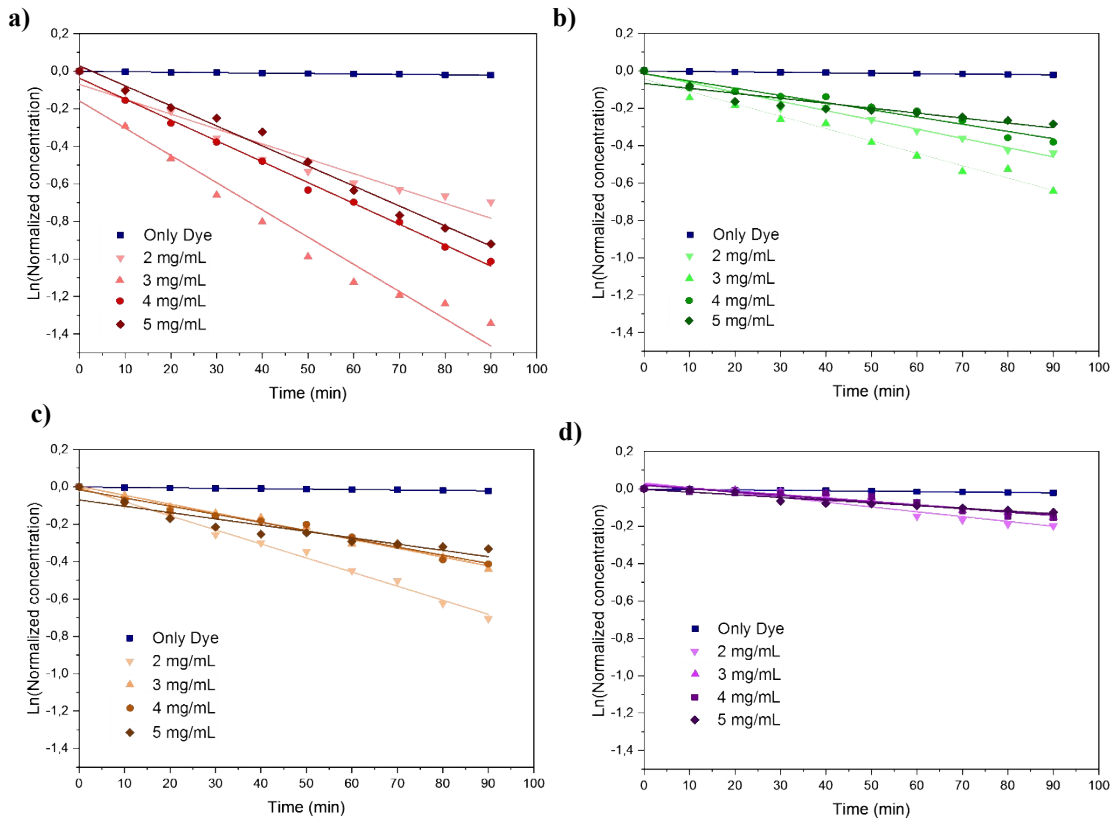

Figure S6. Photodegradation of Toluidine Blue (TB, *ρ(TB) = 55 μg/mL equals c(TB) = 1.80·10*$^{-7}$ *M*) in the presence of (a) N-CDs; (b) N,S-CNs; (c) N,P-CNs; and (d) N,S,P-CNs at different concentration, following a pseudo-first-order kinetics.

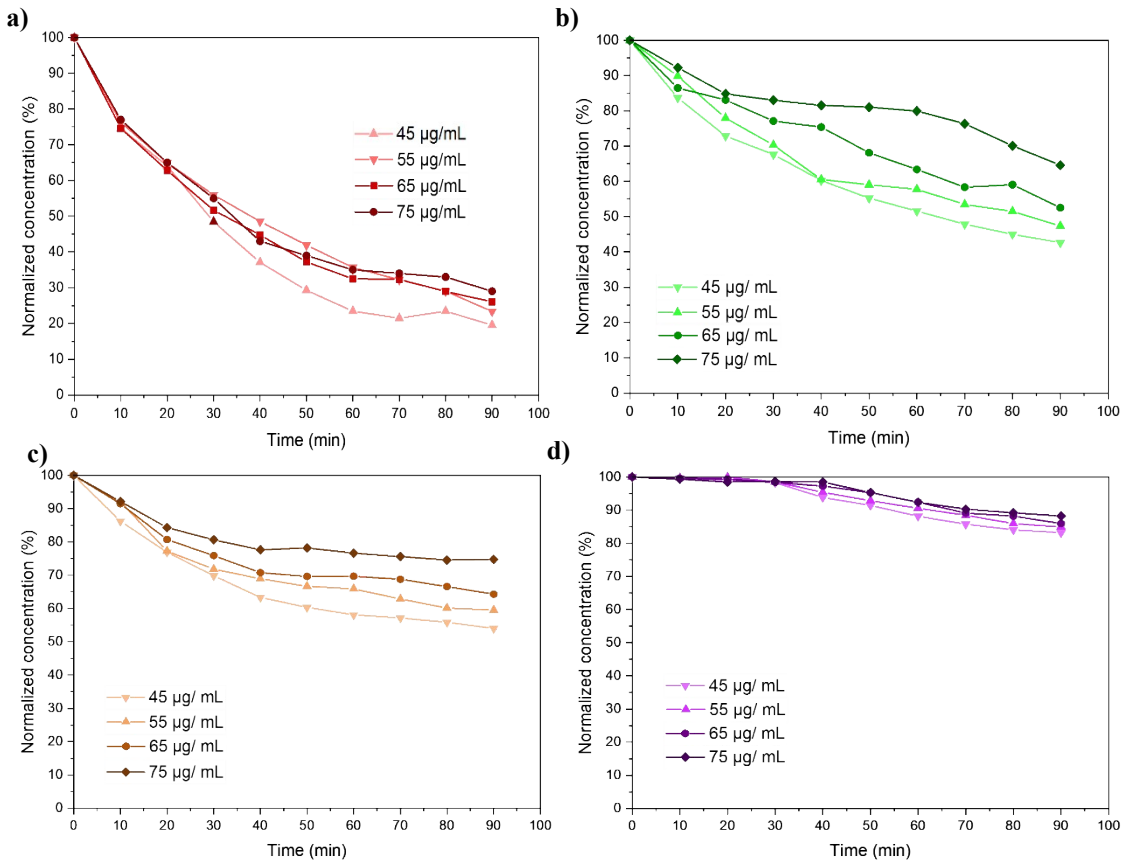

Figure S7. Time evolution of the normalized concentration of Toluidine Blue (TB) at different dye concentrations (*ρ(TB) = 45 µg/mL equals c(TB) = 1.47·10^{-7} M; ρ(TB) = 55 µg/mL equals c(TB) = 1.80·10^{-7} M; ρ(TB) = 65 µg/mL equals c(TB) = 2.13·10^{-7} M; ρ(TB) = 75 µg/mL equals c(TB) = 2.45·10^{-7} M*) in the presence of: (a) N-CDs; (b) N,S-CNs; (c) N,P-CNs; and (d) N,S,P-CNs at a concentration of 3 mg/mL.

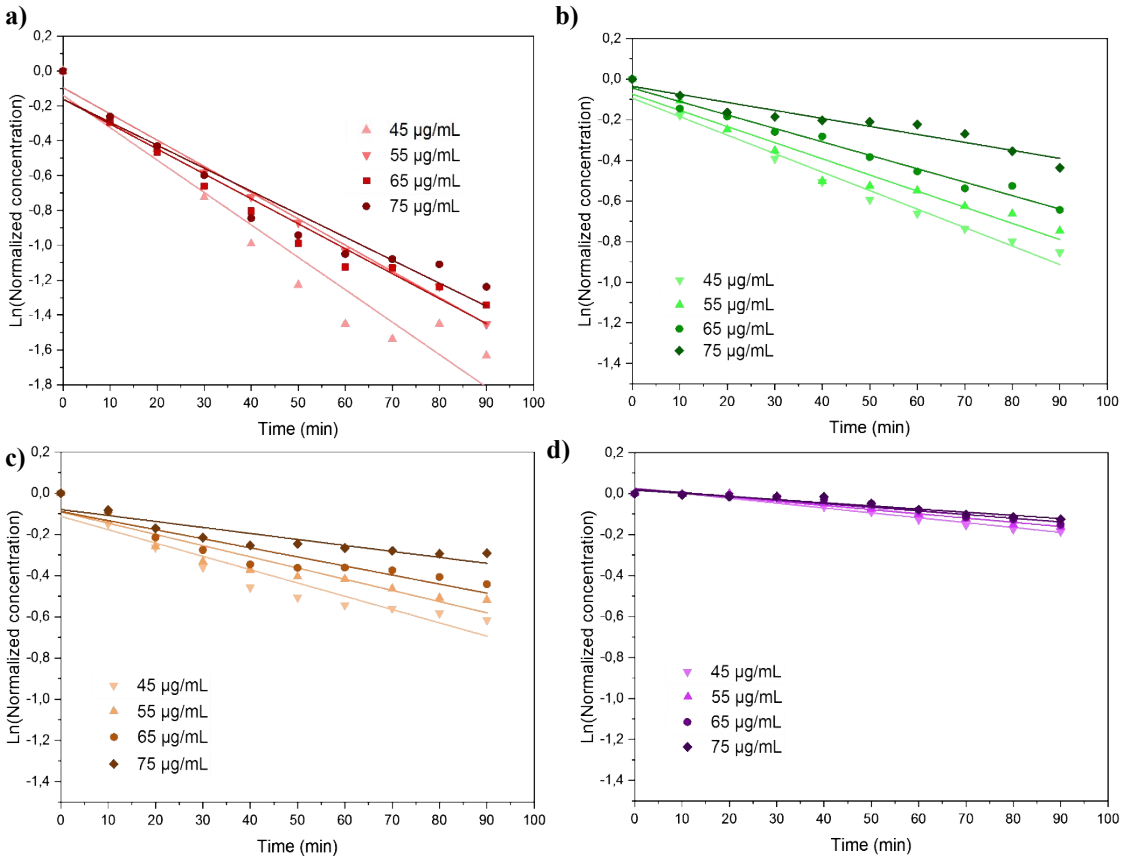

Figure S8. Photodegradation of Toluidine Blue (TB) at different dye concentrations (*ρ(TB) = 45 µg/mL equals c(TB) = 1.47·10^{-7} M; ρ(TB) = 55 µg/mL equals c(TB) = 1.80·10^{-7} M; ρ(TB) = 65 µg/mL equals c(TB) = 2.13·10^{-7} M; ρ(TB) = 75 µg/mL equals c(TB) = 2.45·10^{-7} M*), using 3 mg/mL of (a) N-CDs. (b) N,S-CNs (c) N,P-CNs, (d) N,S,P-CNs. The reactions followed a pseudo-first-order kinetics.

Table S3. Pseudo-first-order rate constants for each doped material at different concentrations; ρ(TB) = 55 μg/mL *equals* c(TB) = $1.80 \cdot 10^{-7}$ M.

TB (dye)	**$(1.4 \pm 0.7) \times 10^{-4}$ k (min^{-1})** (without photocatalysts)			
ρ(photocatalyst)	**2 mg/mL**	**3 mg/mL**	**4 mg/mL**	**5 mg/mL**
N-CDs k (min^{-1})	$(7.9 \pm 0.7) \times 10^{-3}$	$(1.1 \pm 0.1) \times 10^{-2}$	$(1.1 \pm 0.3) \times 10^{-2}$	$(1.1 \pm 0.4) \times 10^{-2}$
N,S-CNs k (min^{-1})	$(4.9 \pm 0.2) \times 10^{-3}$	$(7.0 \pm 0.6) \times 10^{-3}$	$(3.9 \pm 0.3) \times 10^{-3}$	$(2.7 \pm 0.4) \times 10^{-3}$
N,P-CNs k (min^{-1})	$(7.5 \pm 0.2) \times 10^{-3}$	$(8.0 \pm 0.5) \times 10^{-3}$	$(4.4 \pm 0.2) \times 10^{-3}$	$(3.4 \pm 0.5) \times 10^{-3}$
N,S,P-CNs k (min^{-1})	$(2.5 \pm 0.3) \times 10^{-3}$	$(4.0 \pm 0.2) \times 10^{-3}$	$(1.8 \pm 0.2) \times 10^{-3}$	$(1.4 \pm 0.1) \times 10^{-3}$

Table S4. Apparent rate constants for each doped material (ρ(photocatalyst) = 3 mg/mL) at different dye concentrations.

ρ(dye)	**45 µg/mL**	**55 µg/mL**	**65 µg/mL**	**75 µg/mL**
c(dye)	**$1.47 \cdot 10^{-7}$ mol/L**	**$1.80 \cdot 10^{-7}$ mol/L**	**$2.13 \cdot 10^{-7}$ mol/L**	**$2.45 \cdot 10^{-7}$ mol/L**
N-CDs k (min^{-1})	$(1.8 \pm 0.2) \times 10^{-2}$	$(1.5 \pm 0.1) \times 10^{-2}$	$(1.4 \pm 0.1) \times 10^{-2}$	$(1.3 \pm 0.1) \times 10^{-2}$
N,S-CNs k (min^{-1})	$(9.1 \pm 0.5) \times 10^{-3}$	$(7.9 \pm 0.7) \times 10^{-3}$	$(6.6 \pm 0.3) \times 10^{-3}$	$(3.9 \pm 0.4) \times 10^{-3}$
N,P-CNs k (min^{-1})	$(6.5 \pm 0.8) \times 10^{-3}$	$(5.4 \pm 0.7) \times 10^{-3}$	$(4.4 \pm 0.6) \times 10^{-3}$	$(2.9 \pm 0.5) \times 10^{-3}$
N,S,P-CNs k (min^{-1})	$(2.4 \pm 0.2) \times 10^{-3}$	$(2.1 \pm 0.2) \times 10^{-3}$	$(1.8 \pm 0.2) \times 10^{-3}$	$(1.5 \pm 0.2) \times 10^{-3}$

REFERENCES

[1] Miao X, Qu D, Yang D, Nie B, Zhao Y, Fan H, et al. Synthesis of Carbon Dots with Multiple Color Emission by Controlled Graphitization and Surface Functionalization. Adv Mater 2018;30:1704740. https://doi.org/10.1002/adma.201704740.

[2] Nguyen KG, Baragau IA, Gromicova R, Nicolaev A, Thomson SAJ, Rennie A, et al. Investigating the effect of N-doping on carbon quantum dots structure, optical properties and metal ion screening. Sci Rep 2022;12:13806. https://doi.org/10.1038/s41598-022-16893-x.

[3] Wang C, Shi H, Yang M, Yao Z, Zhang B, Liu E, et al. Biocompatible sulfur nitrogen co-doped carbon quantum dots for highly sensitive and selective detection of dopamine. Colloids Surfaces B Biointerfaces 2021;205:111874. https://doi.org/10.1016/j.colsurfb.2021.111874.

[4] Ni P, Li Q, Xu C, Lai H, Bai Y, Chen T. Optical properties of nitrogen and sulfur co-doped carbon dots and their applicability as fluorescent probes for living cell imaging. Appl Surf Sci 2019;494:377–83. https://doi.org/10.1016/j.apsusc.2019.07.196.

[5] Kamali SR, Chen CN, Agrawal DC, Wei TH. Sulfur-doped carbon dots synthesis under microwave irradiation as turn-off fluorescent sensor for Cr(III). J Anal Sci Technol 2021;12. https://doi.org/10.1186/s40543-021-00298-y.

[6] Sun X, Brückner C, Lei Y. One-pot and ultrafast synthesis of nitrogen and phosphorus co-doped carbon dots possessing bright dual wavelength fluorescence emission. Nanoscale 2015;7:17278–82. https://doi.org/10.1039/c5nr05549k.